MCB
Journals.ASM.org

Blockade of the Activin Receptor IIB Activates Functional Brown Adipogenesis and Thermogenesis by Inducing Mitochondrial Oxidative Metabolism

Brigitte Fournier,[a] Ben Murray,[a] Sabine Gutzwiller,[a] Stefan Marcaletti,[a] David Marcellin,[b] Sebastian Bergling,[c] Sophie Brachat,[a] Elke Persohn,[d] Eliane Pierrel,[a] Florian Bombard,[a] Shinji Hatakeyama,[a] Anne-Ulrike Trendelenburg,[e] Frederic Morvan,[a] Brian Richardson,[a] David J. Glass,[e] Estelle Lach-Trifilieff,[a] and Jerome N. Feige[a]

MusculoSkeletal Diseases, Novartis Institutes for Biomedical Research, Basel, Switzerland[a]; Neuroscience, Novartis Institutes for Biomedical Research, Basel, Switzerland[b]; Quantitative Biology, Developmental & Molecular Pathways, Novartis Institutes for Biomedical Research, Basel, Switzerland[c]; Pre-Clinical Safety, Novartis Institutes for Biomedical Research, Basel, Switzerland[d]; and MusculoSkeletal Diseases, Novartis Institutes for Biomedical Research, Cambridge, Massachusetts, USA[e]

Brown adipose tissue (BAT) is a key tissue for energy expenditure via fat and glucose oxidation for thermogenesis. In this study, we demonstrate that the myostatin/activin receptor IIB (ActRIIB) pathway, which serves as an important negative regulator of muscle growth, is also a negative regulator of brown adipocyte differentiation. In parallel to the anticipated hypertrophy of skeletal muscle, the pharmacological inhibition of ActRIIB in mice, using a neutralizing antibody, increases the amount of BAT without directly affecting white adipose tissue. Mechanistically, inhibition of ActRIIB inhibits Smad3 signaling and activates the expression of myoglobin and PGC-1 coregulators in brown adipocytes. Consequently, ActRIIB blockade in brown adipose tissue enhances mitochondrial function and uncoupled respiration, translating into beneficial functional consequences, including enhanced cold tolerance and increased energy expenditure. Importantly, ActRIIB inhibition enhanced energy expenditure only at ambient temperature or in the cold and not at thermoneutrality, where nonshivering thermogenesis is minimal, strongly suggesting that brown fat activation plays a prominent role in the metabolic actions of ActRIIB inhibition.

Metabolic imbalance with caloric input exceeding energy expenditure is one of the hallmarks of metabolic disorders such as obesity and type 2 diabetes. Targeting energy expenditure therefore represents a promising approach to combat these diseases by preventing the detrimental accumulation of fat in peripheral tissues and its negative consequences on insulin sensitivity. In that respect, brown adipose tissue (BAT) is particularly interesting for energy dissipation as its primary function is to convert glucose and fatty acids into heat. The thermogenic potential of brown adipocytes arises from their high mitochondrial density and the specific expression of the uncoupling protein 1 (UCP-1), a mitochondrial protein which generates heat by uncoupling cellular respiration from ATP synthesis (16). The importance of brown fat in humans has recently been reappreciated (25), where the amount and activity of brown fat have been inversely correlated to obesity (6, 40, 42). It has consequently been proposed that increasing the amount and activity of brown fat could be beneficial for treating metabolic diseases where energy intake outcompetes expenditure and leads to an excess of lipid accumulation (5, 16, 26).

Brown adipocytes are found in brown adipose tissue but can also be embedded within white adipose tissue and recruited upon a thermogenic challenge such as cold exposure and β-adrenergic stimulation. Lineage-tracing experiments have shown that BAT specifically shares common developmental origins with skeletal muscle; both of these tissues arise from Myf5-positive precursors which are distinct from those of white adipose tissue (32). In contrast, recruitable brown adipocytes from white adipose tissue have different precursors, as they do not derive from the Myf5 lineage. The demonstration that brown adipocytes from BAT have a myogenic transcriptional and mitochondrial signature (9, 36) further highlights a functional proximity between both tissues. The divergence of the common brown fat/muscle lineage into fully specialized cell types is regulated by PRDM16, which drives the terminal differentiation of brown adipocytes and represses myogenesis (32, 33).

The activin receptor IIB (ActRIIB) integrates the actions of myostatin as well as other transforming growth factor β (TGFβ)-related ligands to negatively regulate skeletal muscle mass (18). ActRIIB dimerizes with Alk4/5 and signals intracellularly via Smad2/3 (37). Genetic deletion of myostatin, ActRIIB, and Smad3 each in mice leads to a significant increase of skeletal muscle (19, 20, 35), which can be recapitulated using pharmacological inhibitors of the pathway in adult animals (11, 17). Ligands of the TGFβ superfamily are also emerging as potent regulators of energy homeostasis (46). Myostatin stimulates the early events of white adipocyte differentiation and inhibits terminal differentiation (22). Myostatin-null mice undergo a reduction in fat mass that is believed to result from their hypermuscularity (12, 23), and myostatin or ActRIIB inhibition can protect from fat accumulation and insulin resistance in various rodent models of metabolic diseases (1, 2, 12, 22, 48).

Given the developmental proximity between BAT and skeletal muscle and the well-established inhibitory actions of myostatin via its receptor, ActRIIB, on the maintenance of muscle mass, we

Received 16 November 2011 **Returned for modification** 20 December 2011
Accepted 7 May 2012
Published ahead of print 14 May 2012
Address correspondence to David J. Glass, david.glass@novartis.com, or Jerome N. Feige, jerome.feige@novartis.com.
Supplemental material for this article may be found at http://mcb.asm.org/.

doi:10.1128/MCB.06575-11

asked whether this pathway influences brown fat differentiation and function. Using combinations of cellular assays and mouse *in vivo* experiments, we demonstrate that the myostatin/ActRIIB pathway represses brown fat homeostasis and activity and can be targeted pharmacologically to activate mitochondrial metabolism and energy expenditure.

MATERIALS AND METHODS

Materials and reagents. All recombinant proteins were from R&D Systems, and the human ActRIIB (hActRIIB; positions 19 to 137)-human Fc (hFc) fusion protein was produced internally. The Fab portion of the monoclonal antibody (Ab) against ActRIIB was isolated by phage display and selected for neutralization of myostatin binding to human, rat, and mouse ActRIIB (see Fig. S1 in the supplemental material). The Fab was then transformed to a human IgG1 or mouse IgG2a format and produced in HEK293 cells. A control human IgG1 was generated against chicken lysozyme. Antibodies against total and phosphorylated Smad3 used for Western blotting were from Cell Signaling and Millipore, respectively.

Reporter gene assay. The Smad2/3 response was evaluated in a $(CAGA)_{12}$-luciferase reporter assay using HEK293T cells stably transfected with pGL3-$(CAGA)_{12}$-Luc. Supernatants from primary brown adipocyte cultures were added on HEK293T-$(CAGA)_{12}$-Luc cells at a final concentration of 90% for 24 h. The Smad1/5/8 response was evaluated in C28a2 cells stably expressing a BMP-responsive element–luciferase construct. Luciferase activity was measured using Britelite Plus reagent (Perkin Elmer).

Brown adipocyte differentiation. Primary brown preadipocytes were isolated from interscapular BAT of 5-week-old male C57BL6/J mice using collagenase dissociation, as described previously (7). Cells were cultured in Dulbecco's modified Eagle medium (DMEM; Invitrogen) supplemented with 10% fetal bovine serum (Sigma), 3 nM insulin (Sigma), and an antibiotic cocktail (Invitrogen). After reaching confluence, brown preadipocytes were differentiated in 12-well plates for 9 days using 20 nM insulin and 1 nM tri-iodothyronine (T3; Sigma) for the entire protocol and 0.5 mM isobutylmethylxanthine (IBMX; Sigma), 0.5 μM dexamethasone (Sigma), and 0.125 mM indomethacin (Sigma) for the first 2 days. Medium and treatments were replaced every 2 days.

Animal experiments. Animal experiments were performed in accordance with the Swiss ordinance on animal experimentation, after approval by cantonal veterinarian authorities. Ten-week-old male C57BL6/J male mice (Janvier Laboratories, France) or CB17/ICR-*Prkdc*^{scid}/Crl female mice (SCID mice; Charles River, Germany) were maintained at 22°C in a 12-h light–12-h dark cycle with unrestricted access to regular diet and water. Animals were treated with the antibodies for 4 weeks by weekly subcutaneous injection at a volume of 5 ml/kg of body weight and a dose of 20 mg/kg, unless otherwise stated. The human IgG1 form was administered to SCID mice to avoid immunogenicity, and the mouse IgG2a form was administered to wild-type (WT) C57BL6/J mice. Cold tolerance was evaluated by placing animals for 4 h at 10°C in individual cages and measuring body temperature every hour with a rectal thermometer (Bioseb). Indirect calorimetry was measured in individual metabolic cages of a comprehensive laboratory animal monitoring system (CLAMS; Columbus Instruments), after a 24-h habituation to the new housing conditions in an independent set of cages. The measurements were performed at room temperature (22°C) on a group of mice that had never been exposed to a cold environment or at 10°C 1 week after the cold tolerance test. In a second experiment, indirect calorimetry was measured at thermoneutrality (30°C) using a Phenomaster system (TSE Systems). Respiration rates were normalized to the body weight of the animal at the start of treatment, and all parameters were integrated over the day and night periods. All animals were sacrificed with CO_2.

Gene expression profiling. RNA was extracted using the TRIzol reagent (Invitrogen). Reverse transcription was performed with random hexamers on 1 μg of total RNA using a high-capacity reverse transcription kit (Applied Biosystems), and the reaction mixture was diluted 100 times for amplification. PCRs were performed in duplicate in 384-well plates on a CFX384 cycler (Bio-Rad) using specific TaqMan probes (Applied Biosystems). Data were normalized to two housekeeping genes using the $\Delta\Delta C_T$ threshold cycle (C_T) method.

Microarray experiments were performed using Affymetrix mouse A430_2 chips according to the manufacturer's instructions. Gene set enrichment analysis was performed with an internal implementation of the methodologies described previously (27, 34). The set of genes upregulated in the muscle of PGC-1α transgenic mice was generated from microarray data in muscle-specific PGC-1α transgenic mice (4).

Histology. Hematoxylin-eosin (H&E) staining was performed on tissues fixed in 4% paraformaldehyde after they were embedded in paraffin and sectioned as described previously (7), and micrographs were taken on a wide-field microscope with a color charge-coupled-device camera (Olympus). Lipid droplet size was quantified from H&E images using software developed internally. Laminin and UCP-1 immunohistochemistries were performed on paraffin-embedded sections with primary antibodies from Sigma and Abcam, respectively, and a horseradish peroxidase-conjugated secondary antibody which was incubated with DAB (3,3′-diaminobenzidine; Vector Biolabs) for 16 S. The size of brown adipocytes within interscapular BAT was quantified from 3 independent pictures of the laminin staining per animal, using Cell P software (Olympus). For electron microscopy, BAT was fixed with 3% glutaraldehyde in 0.1 M cacodylate buffer, pH 7.4, for 1 h at 4°C and 1% OsO_4 in 0.1 M cacodylate buffer, pH 7.4, for 1 h at 4°C. After postfixation, the tissues were dehydrated in graded acetone solutions and embedded in Epon. Ultrathin sections were counterstained with uranyl acetate and lead citrate and examined with a Philips Technai transmission electron microscope.

Cellular oxygen consumption. Oxygen consumption was measured on a Seahorse Bioscience XF24 analyzer as described previously (7). Oligomycin (final concentration, 2.5 μg/ml; Calbiochem) and FCCP [carbonylcyanide-*p*-(trifluoromethoxy)-phenylhydrazone, final concentration, 500 nM; Sigma-Aldrich] were injected during the assay to measure uncoupled and maximal respiration, respectively.

Statistical analysis. All results are presented as mean ± standard error of the mean (SEM) and were analyzed using one- or two-way analysis of variance (ANOVA) or unpaired two-tailed Student's *t* test according to the experimental design. Values were considered statistically significant at a P value of <0.05.

RESULTS

The role of myostatin and ActRIIB on brown adipose homeostasis was first evaluated using brown adipocyte differentiation in a primary cellular model, where brown preadipocytes were isolated from mouse interscapular BAT and differentiation was induced with a classical brown adipogenic cocktail. As expected, the adipogenic medium induced lipid accumulation (Fig. 1A) and activated the expression of mature brown adipocyte markers while repressing preadipocyte markers (Fig. 1B, subsets 1 and 2, respectively). Myostatin treatment strongly impaired the ability of brown adipocytes to differentiate, and this effect was reversed by a monoclonal antibody preventing the binding of myostatin to the ActRIIB receptor (Fig. 1A). This was confirmed at the molecular level, as many genes induced during brown adipogenesis, including prototypical brown fat markers such as UCP-1, CIDEA, or Elovl3, were inhibited by myostatin and reversed by the ActRIIB Ab (Fig. 1B and C; see Fig. S2 in the supplemental material). In addition, the ActRIIB Ab strongly exacerbated the expression of a large subset of mature brown adipocyte genes even in the absence of myostatin (Fig. 1B, subset 1a; see Fig. S2 in the supplemental material), suggesting the presence of endogenous inhibitory ActRIIB ligands that regulate brown fat tone. To test this possibility, the supernatants from preadipocytes and differentiated brown

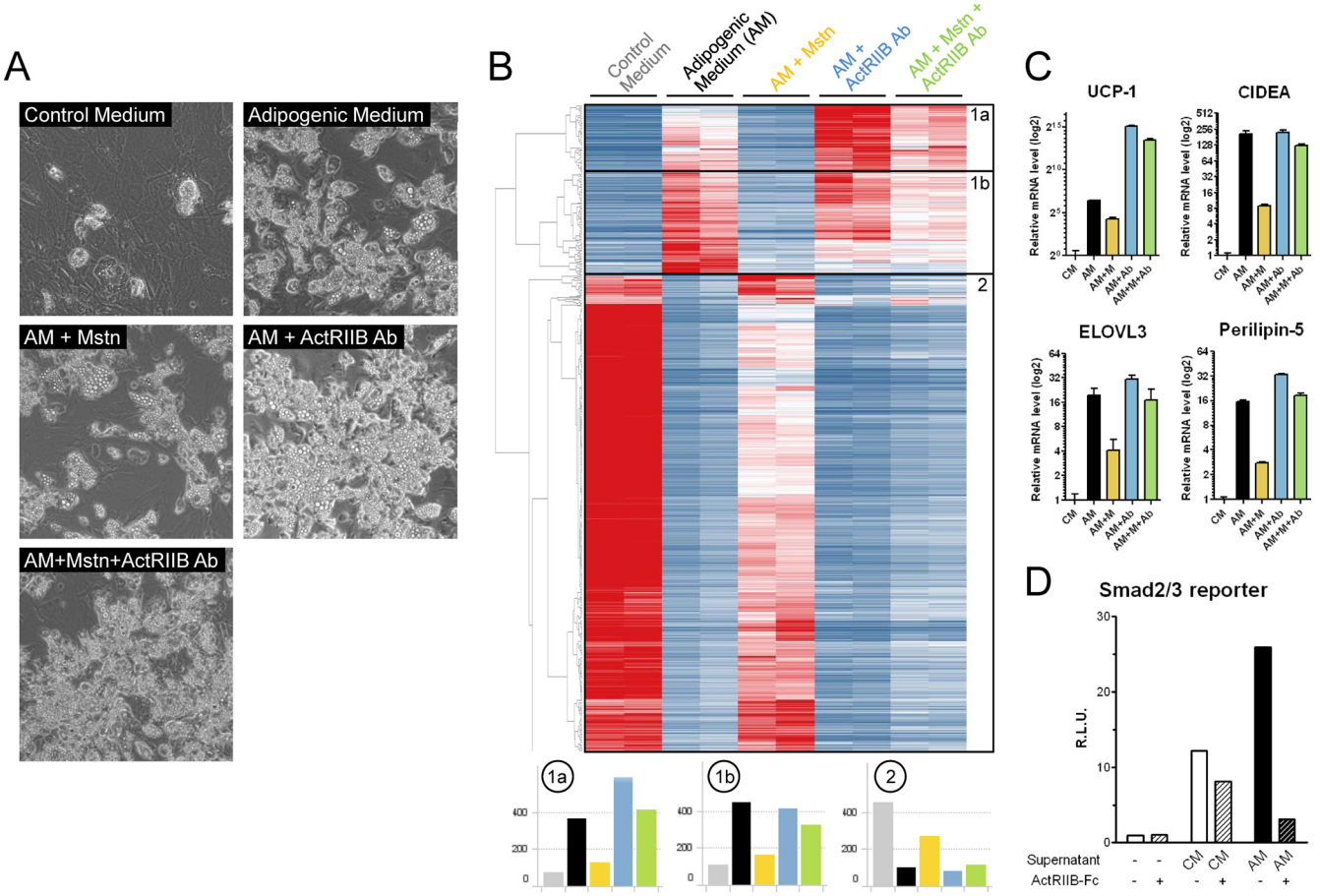

FIG 1 The activin receptor IIB inhibits the differentiation of primary brown adipocytes. (A to C) Primary brown preadipocytes isolated from mouse interscapular BAT were differentiated for 9 days using a classical adipogenic medium (AM) containing insulin and thyroid hormone for the entire protocol and IBMX, dexamethasone, and indomethacin for the first 2 days. Myostatin (Mstn or M; 10 ng/ml), a monoclonal antibody against the activin receptor IIB (ActRIIB Ab; 10 μg/ml), or a combination of both were added to the adipogenic medium, and fresh medium and treatments were replaced every 2 days. The level of differentiation was evaluated by visualizing lipid droplet accumulation using phase-contrast light microscopy (A) and by a nonbiased clustering analysis of expression microarray data from 2 independent cultures for each condition (B). The heat map in panel B is colorized according to gene expression from dark blue (low expression) to dark red (high expression). The average expression of all genes in clusters 1a, 1b, and 2 is represented below the heat map. (C) The expression of classical brown fat markers was measured by quantitative reverse transcription-PCR. (D) The supernatants from the primary brown adipocytes treated with control medium (CM) and adipogenic medium were subjected to a Smad2/3 reporter gene assay where a $(CAGA)_{12}$-luciferase reporter was stably transfected into HEK293 T cells. The ActRIIB-dependent response was determined by adding an ActRIIB-Fc at 10 μg/ml. R.L.U., relative luciferase units.

adipocytes were analyzed using a Smad2/3 reporter gene assay which integrates TGFβ, activin, and myostatin signaling (46). The Smad2/3 reporter was activated by the supernatant from brown preadipocytes but further enhanced by the supernatant from differentiated brown adipocytes (Fig. 1D). The Smad2/3 response induced by the supernatant from differentiated brown adipocytes was mainly driven by ActRIIB ligands, as it was almost totally abolished when ActRIIB was inhibited using a soluble ActRIIB-Fc receptor. To evaluate if ActRIIB integrates multiple ligands in brown fat, we also treated primary brown adipocytes with other ligands of the TGFβ superfamily signaling via ActRIIB and Alk4/5. Similar to the results obtained with myostatin, activin A and, to a lesser extent, activin B were potent inhibitors of brown adipogenesis, whereas GDF-11 was not effective (see Fig. S3 in the supplemental material). Together, these results demonstrate that ActRIIB ligands are produced during brown adipogenesis and negatively regulate differentiation and that ActRIIB blockade with a neutralizing antibody can release this inhibition to enhance brown adipocyte differentiation.

To evaluate how ActRIIB and its ligands regulate brown adipose tissue *in vivo*, the ActRIIB antibody was administered to WT mice for 4 weeks. ActRIIB inhibition increased the mass of interscapular BAT dose dependently, reaching a 40% increase compared to control when the antibody was injected at 20 mg/kg/week (Fig. 2A). Consistent with other studies showing no effect of postnatal myostatin inhibition on white fat in the absence of an obesogenic challenge (1, 22, 44), increased fat mass in mice treated with the ActRIIB Ab was specific for brown fat, since the amount of white adipose tissue was not affected after 4 weeks of treatment with the Ab. As expected, given data from previous genetic or pharmacological ActRIIB inhibition (19, 20), the ActRIIB Ab also increased the mass of skeletal muscle, which demonstrates that the increase in brown fat is not occurring at the expense of skeletal muscle. Larger amounts of brown fat in ActRIIB Ab-treated mice correlated with an increase in the size of brown, but not white, adipocytes at the histological level (Fig. 2B to D). Inhibition of ActRIIB did not affect the recruitable brown adipocytes localized within white adipose tissue, as the ActRIIB Ab did not increase the

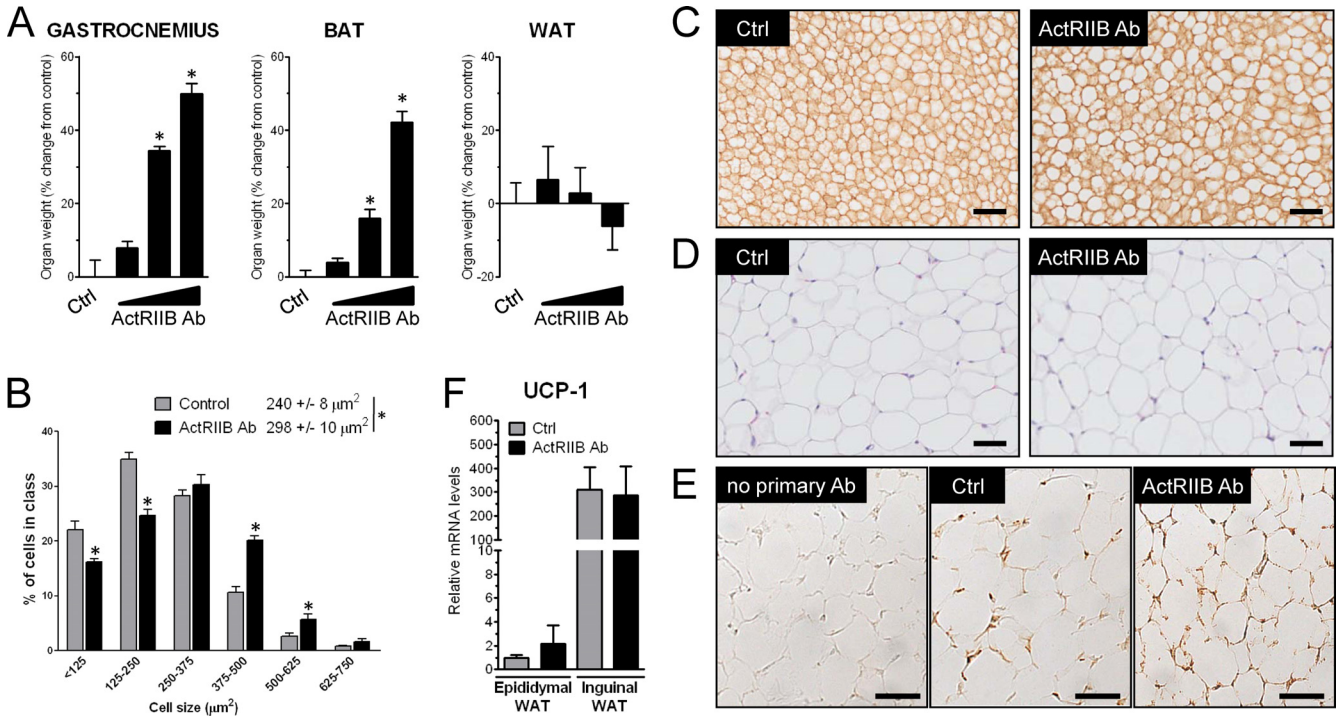

FIG 2 ActRIIB inhibition in mice increases the amount of brown but not white fat. (A) SCID mice ($n = 12$/group) were treated for 4 weeks with a weekly subcutaneous injection of control (Ctrl) antibody (IgG1; 20 mg/kg/week) or increasing amounts of a human monoclonal antibody against ActRIIB (2, 6, and 20 mg/kg/week). The wet mass of gastrocnemius muscle, interscapular BAT, and epididymal white adipose tissue (WAT) was measured and expressed as the percent change from the average of the control group. *, $P < 0.05$. (B and C) Interscapular brown adipose tissue from control and ActRIIB Ab-treated mice (20 mg/kg/week) was imaged by light microscopy after laminin staining, and cell size was quantified by histomorphometry. (D) Epididymal white adipose tissue from control and ActRIIB Ab-treated mice (20 mg/kg/week) was imaged by light microscopy after hematoxylin-eosin staining. (E) Inguinal white adipose tissue from control and ActRIIB Ab-treated mice (20 mg/kg/week) was imaged by light microscopy after UCP-1 immunohistochemistry. Bars, 50 μm. (F) Quantitative reverse transcription-PCR measurement of relative UCP-1 levels in epididymal and inguinal white adipose tissue from control and ActRIIB Ab-treated mice (20 mg/kg/week).

pool of UCP-1-positive brown adipocytes in inguinal white adipose tissue, a white fat depot with a high propensity to browning (Fig. 2E). This was confirmed at the molecular level, as UCP-1 levels were not affected in either epididymal or inguinal white adipose tissue (Fig. 2F). The two main cellular determinants of BAT are the presence of lipid droplets acting as a local reservoir of energy and a high density of mitochondria accounting for the high metabolic rate required for heat production (8). Histological analysis of BAT from ActRIIB Ab-treated mice revealed an increase of the size of lipid droplets (Fig. 3A). This observation was further corroborated at higher magnification using electron microscopy; however, the amount and density of mitochondria in brown fat were not significantly affected by the ActRIIB Ab (Fig. 3B and C).

At the molecular level, the ActRIIB Ab prevented Smad3 phosphorylation in brown adipose tissue, indicating that the receptor transduced signals in brown fat similarly to the way that it does in skeletal muscle (Fig. 4A). In order to characterize the molecular signature of the ActRIIB Ab in brown fat downstream of Smad3, gene expression was measured by microarray and functionally clustered using gene set enrichment analysis. Treatment with the ActRIIB Ab significantly induced the expression of multiple sets of genes governing oxidative metabolism and mitochondrial function (Fig. 4B), two processes that are key for high energy expenditure via enhanced thermogenesis. Interestingly, the molecular fingerprint of the ActRIIB Ab in brown fat overlapped with that observed upon overexpression of PGC-1α, a major regulator of oxidative metabolism and mitochondrial function (13). At the single-gene level, myostatin treatment in primary brown adipocytes inhibited the expression of PGC-1α and PGC-1β as well as downstream mitochondrial proteins, such as UCP-1 and Cox7a1, which are required for brown fat function (Fig. 4C). Consistently, these genes were also strongly activated upon ActRIIB inhibition. We also uncovered a similar regulation of myoglobin expression, which was strongly activated by the ActRIIB Ab and inhibited by myostatin (Fig. 4C). Myoglobin is a gene essential for oxygenation of skeletal muscle (28) for which no role in brown fat function has been previously described. However, the high expression of myoglobin in brown adipose tissue, combined with its induction during brown adipogenesis and cold exposure (see Fig. S4 in the supplemental material), makes it a possible candidate to explain how oxygen is supplied to mitochondria to sustain high respiration rates in brown adipocytes. Altogether, these results demonstrate that ActRIIB inhibition promotes the growth and activation of brown adipose tissue through an atypical mechanism involving brown adipocyte hypertrophy and mitochondrial activation.

BMPs are positive regulators of adipogenesis that can also bind to ActRIIB, with BMP-2 and -4 promoting white adipogenesis (31), while BMP-7 drives brown adipogenesis (38). In contrast to myostatin, which signals via Smad2/3 using Alk4/5 as a corecep-

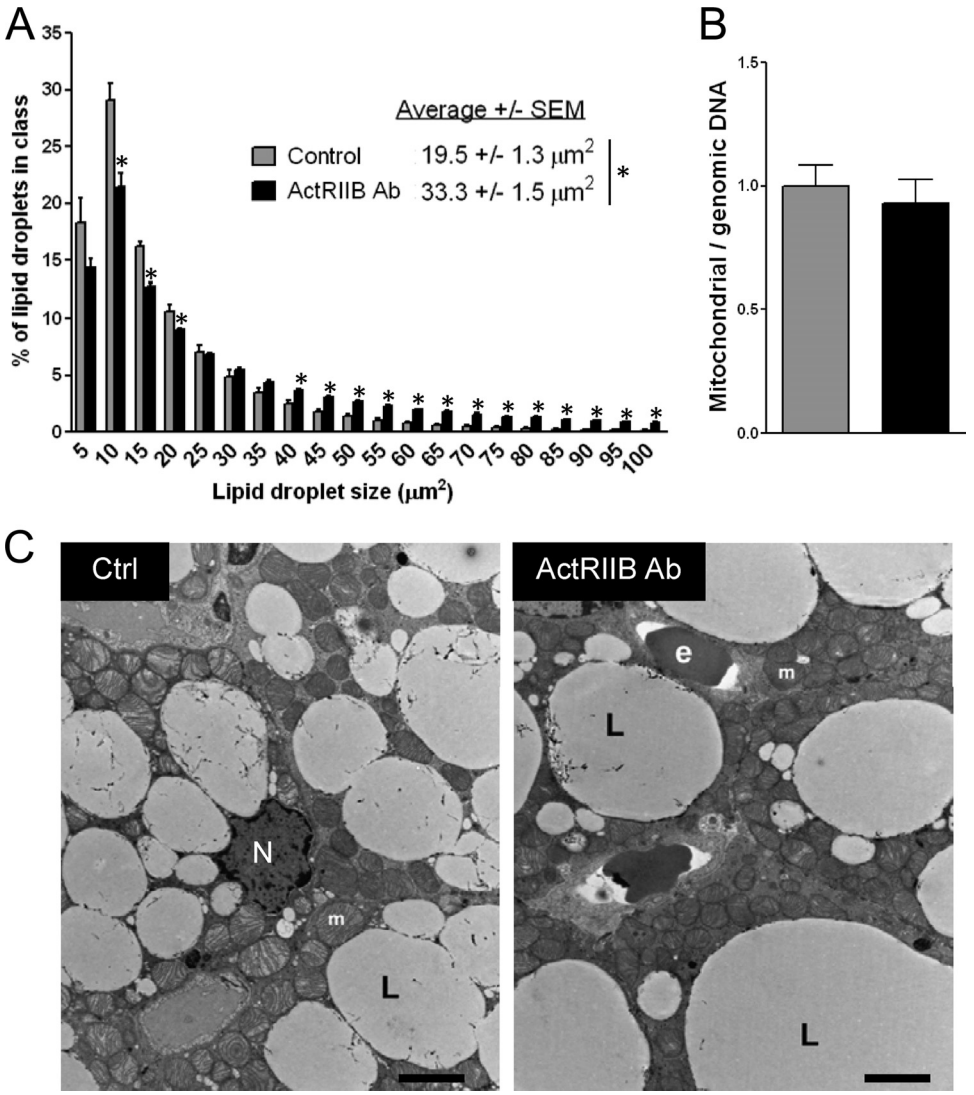

FIG 3 ActRIIB inhibition increases lipid but not mitochondrial density. (A) Lipid droplet size was analyzed on hematoxylin-eosin-stained sections from interscapular BAT using automated detection and quantification software (n = 5/group). *, $P < 0.05$. (B) Mitochondrial DNA was quantified after DNA extraction by amplifying the mitochondrial gene cytochrome *b* by TaqMan quantitative PCR and normalizing to the levels of two probes detecting genomic DNA. (C) Interscapular brown adipose tissue from control and ActRIIB Ab-treated mice (20 mg/kg/week) was imaged by electron microscopy (C). L, lipid droplet; e, erythrocyte; N, nucleus, m, mitochondrion. Bars, 0.5 μm.

tor, BMP signals through a Smad1/5/8 response driven by Alk2/3-, and BMP-7 signaling is inhibited by myostatin (30) (Fig. 5A). We initially speculated that the ActRIIB Ab may promote its biological effects in brown fat through specific permissivity for BMP-7 but not myostatin, thereby enhancing BMP-7 signaling by blocking the inhibitory action of myostatin on the ActRIIB-Alk2/3 complex. However, the effects of the ActRIIB Ab on brown fat most likely do not involve enhanced BMP signaling, as the ActRIIB Ab also inhibits BMP-2, -4, and -7 signaling on Smad1/5/8 (Fig. 5A). In addition, the activation of brown fat markers observed upon BMP-7 treatment and ActRIIB inhibition are not additive (Fig. 5B). Interestingly, we observed that BMP-2, -4, and -7 inhibit myostatin signaling on Smad2/3 (Fig. 5A). Given the inhibitory actions of myostatin on brown adipogenesis and brown fat function, it is possible that some of the beneficial effects of BMP7 on brown fat (38) are mediated by inhibition of myostatin signaling.

The influence of ActRIIB inhibition on the functionality of BAT was next evaluated *in vivo* by exposing mice to a cold environment, which activates the thermogenic potential of brown fat. Mice treated with the ActRIIB Ab were significantly protected from hypothermia upon cold exposure (Fig. 6A), demonstrating that ActRIIB inhibition enhances adaptive thermogenesis. Since BAT is an important site of energy dissipation, especially during cold exposure, whole-body energy expenditure was evaluated using indirect calorimetry either at room temperature or in the cold. Treatment with the ActRIIB Ab increased both basal and cold-induced oxygen consumption and carbon dioxide release but did not affect food intake or the utilization of lipids versus carbohydrates as metabolic substrates, as the ratio of carbon dioxide produced to oxygen consumed (VCO_2/VO_2) was unaffected by the treatment (Fig. 6B; see Fig. S5 in the supplemental material). These experiments were conducted in an experimental setting

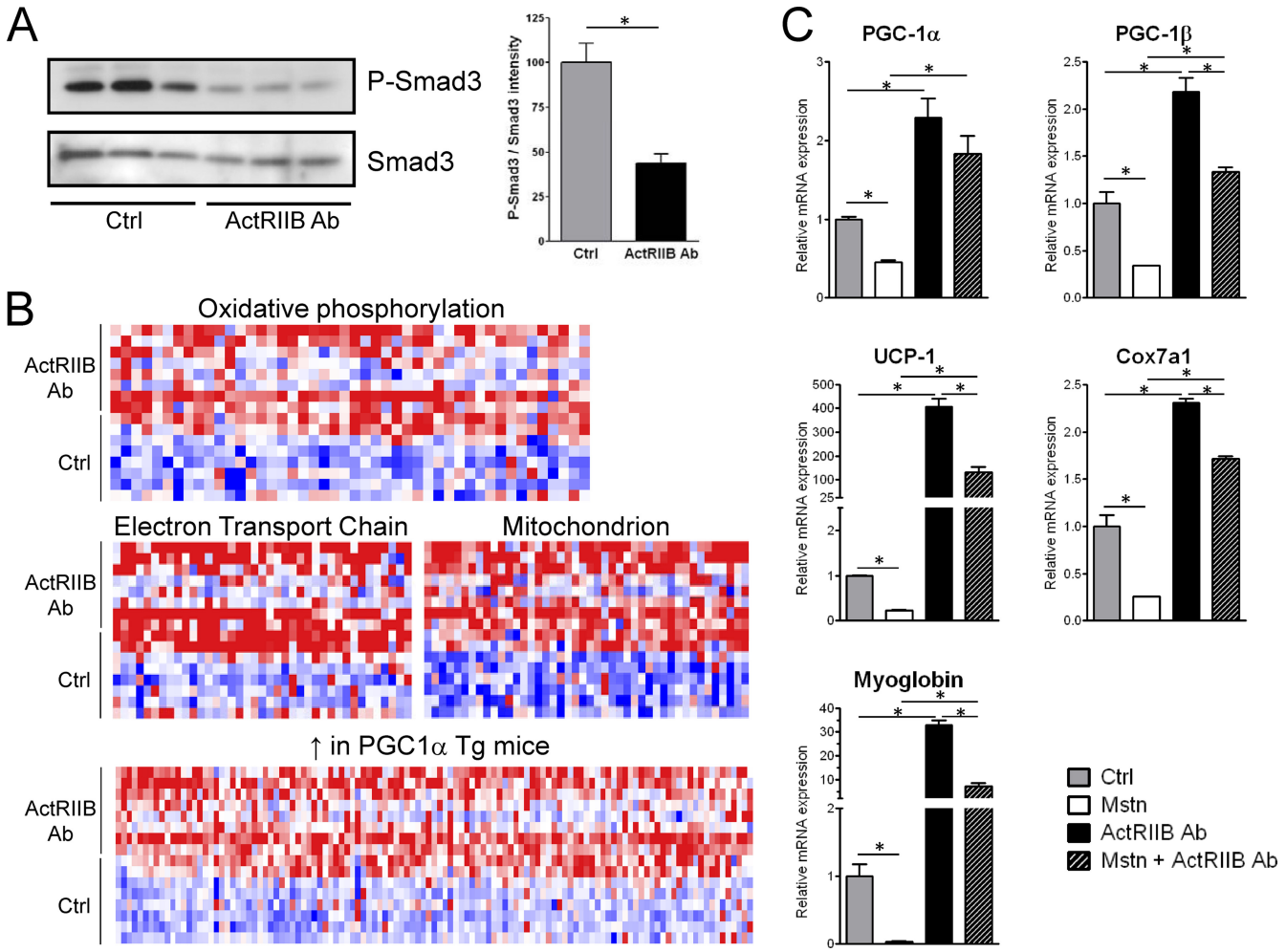

FIG 4 ActRIIB inhibition blocks Smad3 phosphorylation in BAT and activates oxidative metabolism. (A) Total and phosphorylated Smad3 protein levels in interscapular BAT of WT mice treated with IgG1 or the ActRIIB antibody at 20 mg/kg/week were measured by Western blotting. The quantification of two independent experiments is shown on the right. (B) Gene set enrichment analysis following microarray analysis of interscapular BAT of mice treated with IgG1 or the ActRIIB antibody at 20 mg/kg/week. Expression values were ranked and colorized from dark blue for low expression to dark red for high expression. Tg, transgenic. (C) Primary brown adipocytes were treated with myostatin (Mstn; 10 ng/ml), the ActRIIB Ab (10 μg/ml), or a combination of both, and gene expression was measured by quantitative reverse transcription-PCR using specific TaqMan probes for the indicated genes. *, $P < 0.05$.

where muscle hypertrophy did not exceed 15% to minimize potential confounding effects through shivering. We then performed indirect calorimetry at thermoneutrality (30°C) to blunt the nonshivering thermogenesis occurring primarily in brown fat. As previously reported, thermoneutrality decreased the metabolic rate of control mice by about 30 to 35% (10). The elevation of oxygen consumption and carbon dioxide release upon ActRIIB inhibition at ambient temperature was fully inhibited when the measurement was done at thermoneutrality (Fig. 6C), strongly suggesting that the effects of ActRIIB inhibition on energy expenditure primarily arise from activation of nonshivering thermogenesis in brown fat. To further determine whether ActRIIB inhibition directly enhances the metabolic rate of brown fat, cellular respiration was measured in primary brown adipocytes treated with the ActRIIB Ab or with myostatin. Uncoupled respiration, which is responsible for the thermogenic effects of brown adipocytes, and maximal respiration induced by a chemical uncoupler were significantly decreased by myostatin and were increased by the ActRIIB Ab (Fig. 6D). Inhibition of ActRIIB therefore enhances uncoupled respiration of brown adipocytes and thereby increases thermogenesis and energy expenditure of the entire animal at least in part via brown fat activation.

DISCUSSION

A developmental and functional link between skeletal muscle and brown adipose tissue has emerged over the past few years (9, 32, 36). Our results demonstrate that this link also extends at the level of signaling pathways which specifically regulate the homeostasis of both tissues. Indeed, myostatin and its receptor ActRIIB not only are strong inhibitors of muscle mass, as already widely documented, but also are potent regulators of brown adipogenesis and BAT function, without directly affecting white adipose tissue. Consistent with a study published during the revision of the manuscript (15), we observed that myostatin strongly inhibits brown adipocyte differentiation and that this inhibition is reversed by a neutralizing antibody against ActRIIB. In addition, brown adipocytes readily secrete ActRIIB ligands which inhibit differentiation in an autocrine fashion. Pharmacological inhibition of

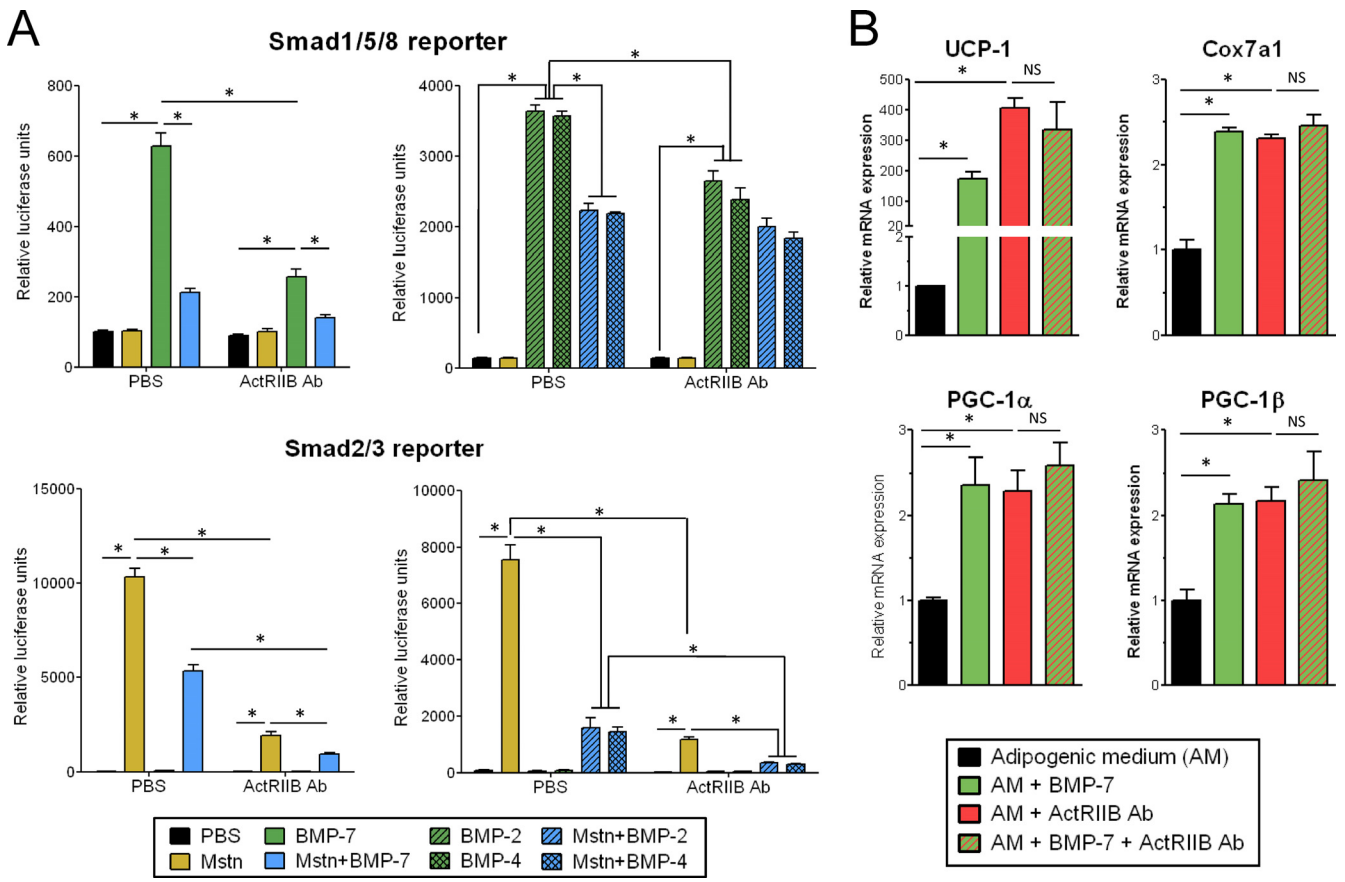

FIG 5 The ActRIIB antibody does not potentiate BMP signaling. (A) Smad1/5/8 activity was measured using a BMP response element-luciferase reporter stably expressed in C28a2 cells, and Smad2/3 activity was measured with a $(CAGA)_{12}$-luciferase reporter stably expressed in HEK293 cells. BMP-2, -4, and -7 were incubated at 200, 100, and 200 ng/ml, respectively, myostatin was incubated at 100 ng/ml, and the ActRIIB antibody was incubated at 10 μg/ml. PBS, phosphate-buffered saline. (B) Primary brown adipocytes were treated with BMP-7 (3 nM), the ActRIIB Ab (10 μg/ml), or a combination of both, as described in the legend to Fig. 1. *, $P < 0.05$; NS, not significant.

ActRIIB is therefore sufficient to enhance brown adipocyte differentiation and to induce the growth and activation of brown adipose tissue *in vivo*. The activation of brown fat function is evidenced by the activation of oxidative metabolism and increased uncoupled respiration in animals treated with an ActRIIB antibody. Given the overlap of the molecular signatures induced by PGC-1α overexpression and ActRIIB inhibition *in vivo*, the activation of PGC-1α and PGC-1β likely plays an important role in inducing the gene expression programs required to enhance mitochondrial function and thermogenesis, as these coregulators play a crucial role in determining the metabolic and thermogenic potential of brown adipocytes (29, 39). The ActRIIB Ab induces oxidative metabolism and thermogenesis in brown fat without changes in mitochondrial density, most likely because the levels of PGC-1 activation upon ActRIIB inhibition are not strong enough to drive the full program of mitochondrial biogenesis or because PGC-1 regulators integrate posttranslational modification to drive specific subsets of biological functions, as recently demonstrated in liver (21).

PRDM16 is a molecular switch that controls the fate of common muscle/brown fat precursors by driving the differentiation of brown adipogenesis and repressing myogenesis (14, 32). However, the regulation of brown fat differentiation and function by ActRIIB most likely involves a mechanism independent of PRDM16, as PRDM16 expression was not significantly affected by the ActRIIB Ab (data not shown) and ActRIIB inhibition promotes an anabolic response in brown fat and skeletal muscle concomitantly. Irisin is a novel myokine which promotes the activation of brown adipocytes within white adipose tissue upon secretion by skeletal muscle in response to exercise (3). We observed that the inhibition of ActRIIB increases the amount and activity of brown fat without amplifying the brown adipocyte pool of white fat. In addition, the irisin precursor Fndc5 was not regulated by the ActRIIB antibody in skeletal muscle (data not shown) and the ActRIIB Ab could induce cell autonomous activation of cultured brown adipocytes, making it unlikely that our observations result from a muscle-brown fat cross talk via irisin. Browning of white fat is also observed upon deletion of Smad3 (45), for which both TGFβ signaling and myostatin signaling are important (45, 48). Despite reducing Smad3 phosphorylation in BAT, we did not detect browning of white fat in mice treated with the ActRIIB Ab. This may be due to differential tuning of Smad2/3 activity by various TGFβ and ActRIIB ligands and to the complex interplay between these ligands and their receptors and coreceptors in brown versus white fat. Our results highlight that multiple ActRIIB ligands, including myostatin and activins, negatively reg-

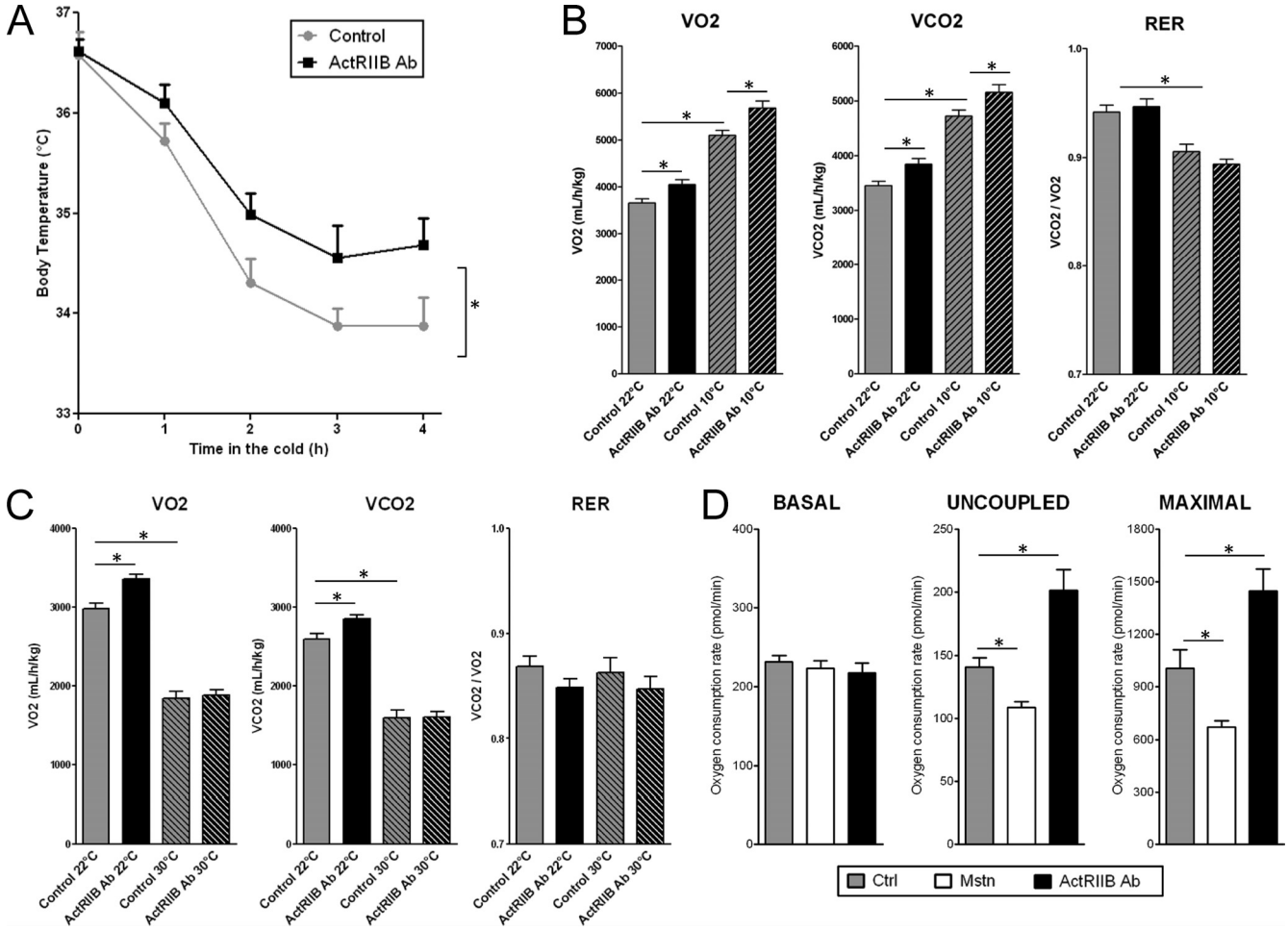

FIG 6 ActRIIB inhibition increases cold tolerance and energy expenditure via nonshivering thermogenesis. (A) Cold tolerance was evaluated by placing C57BL6/J mice ($n = 11$/group) that had been treated for 3 weeks with a weekly subcutaneous injection of vehicle or a mouse monoclonal antibody against ActRIIB (20 mg/kg/week) at 10°C for 4 h and measuring rectal body temperature every hour. (B and C) Energy expenditure was measured for 20 to 24 h by indirect calorimetry for mice treated as described for panel A for 4 weeks. Measurements were performed at 22°C, 10°C (cold), or 30°C (thermoneutrality) for independent groups of mice ($n = 8$ to 11/group). Data were integrated over the dark (B) or the light (C) phase to maximize the effects of temperature. (D) The oxygen consumption rate in primary brown adipocytes treated with myostatin (Mstn; 10 ng/ml) or the ActRIIB Ab (10 μg/ml) ($n = 10$ per condition) was measured under basal conditions or in the presence of oligomycin (uncoupled) or FCCP (maximal). *, $P < 0.05$.

ulate brown adipocyte differentiation and thermogenesis, while the actions of the ActRIIB Ab in brown fat do not seem to include cross talk with BMP-7 signaling. The fact that BMP-7 inhibits myostatin signaling on Smad2/3 actually suggests that some of the effects of BMP-7 in brown fat (38) could arise from inhibition of myostatin. However, the improved metabolic profile in mice deficient for follistatin-like 3, an endogenous inhibitor of myostatin and activins, suggests that some TGFβ-like ligands may positively control energy homeostasis via independent mechanisms, such as a positive effect on pancreatic β cells (24).

Given the prominent role of brown fat in the control of energy expenditure, our results demonstrating that therapeutic inhibition of ActRIIB can enhance the amount and function of brown adipose tissue demonstrate that the regulation of the myostatin/ActRIIB pathway in brown fat plays an important role in controlling energy homeostasis. Since brown fat-enhancing therapies have a strong potential in the treatment of metabolic disorders (41), increased brown fat function most likely contributes to the protection from obesity and type 2 diabetes in various experimental settings (1, 2, 12, 23) where myostatin and ActRIIB are inhibited. Importantly, the possibility to concomitantly restore muscle mass and strength and to enhance energy expenditure via brown fat activation is particularly attractive in old populations where sarcopenia and muscle dysfunction often coincide with obesity and its associated detrimental effects on glucose homeostasis and locomotion (43, 47).

ACKNOWLEDGMENTS

We thank the Muscle Diseases Group at the Novartis Institutes for Biomedical Research (NIBR) for their enthusiastic support, along with the rest of the NIBR community, in particular, Mark Fishman, Michael Rebhan, and the cellular imaging and discovery pathology groups. We also thank Chris Lu and KellyAnn Sheppard for their contribution in the identification of the ActRIIB antibody; Zhidan Wu, Yunyu Zhang, Olivia Bare, and Shilpa Kadam for the generation of technical tools to study PGC-1/UCP-1; and Thomas Suply and the phenotyping unit of the Ecole Polytechnique Federale de Lausanne for access to phenotyping equipment.

All authors are employees of Novartis Pharma AG.

REFERENCES

1. **Akpan I, et al.** 2009. The effects of a soluble activin type IIB receptor on obesity and insulin sensitivity. Int. J. Obes. (Lond.) **33**:1265–1273.
2. **Bernardo BL, et al.** 2010. Postnatal PPARdelta activation and myostatin inhibition exert distinct yet complimentary effects on the metabolic profile of obese insulin-resistant mice. PLoS One **5**:e11307. doi:10.1371/journal.pone.0011307.
3. **Bostrom P, et al.** 2012. A PGC1-alpha-dependent myokine that drives brown-fat-like development of white fat and thermogenesis. Nature **481**: 463–468.
4. **Calvo JA, et al.** 2008. Muscle-specific expression of PPARgamma coactivator-1alpha improves exercise performance and increases peak oxygen uptake. J. Appl. Physiol. **104**:1304–1312.
5. **Cypess AM, Kahn CR.** 2010. Brown fat as a therapy for obesity and diabetes. Curr. Opin. Endocrinol. Diabetes Obes. **17**:143–149.
6. **Cypess AM, et al.** 2009. Identification and importance of brown adipose tissue in adult humans. N. Engl. J. Med. **360**:1509–1517.
7. **Feige JN, et al.** 2008. Specific SIRT1 activation mimics low energy levels and protects against diet-induced metabolic disorders by enhancing fat oxidation. Cell Metab. **8**:347–358.
8. **Feldmann HM, Golozoubova V, Cannon B, Nedergaard J.** 2009. UCP1 ablation induces obesity and abolishes diet-induced thermogenesis in mice exempt from thermal stress by living at thermoneutrality. Cell Metab. **9**:203–209.
9. **Forner F, et al.** 2009. Proteome differences between brown and white fat mitochondria reveal specialized metabolic functions. Cell Metab. **10**:324–335.
10. **Golozoubova V, et al.** 2004. Depressed thermogenesis but competent brown adipose tissue recruitment in mice devoid of all hormone-binding thyroid hormone receptors. Mol. Endocrinol. **18**:384–401.
11. **Goncalves MD, et al.** 2010. Akt deficiency attenuates muscle size and function but not the response to ActRIIB inhibition. PLoS One **5**:e12707. doi:10.1371/journal.pone.0012707.
12. **Guo T, et al.** 2009. Myostatin inhibition in muscle, but not adipose tissue, decreases fat mass and improves insulin sensitivity. PLoS One **4**:e4937. doi:10.1371/journal.pone.0004937.
13. **Handschin C, Spiegelman BM.** 2006. Peroxisome proliferator-activated receptor gamma coactivator 1 coactivators, energy homeostasis, and metabolism. Endocr. Rev. **27**:728–735.
14. **Kajimura S, et al.** 2009. Initiation of myoblast to brown fat switch by a PRDM16-C/EBP-beta transcriptional complex. Nature **460**:1154–1158.
15. **Kim WK, et al.** 2012. Myostatin inhibits brown adipocyte differentiation via regulation of Smad3-mediated beta-catenin stabilization. Int. J. Biochem. Cell Biol. **44**:327–334.
16. **Kozak LP, Anunciado-Koza R.** 2008. UCP1: its involvement and utility in obesity. Int. J. Obes. (Lond.) **32**(Suppl 7):S32–S38.
17. **LeBrasseur NK, et al.** 2009. Myostatin inhibition enhances the effects of exercise on performance and metabolic outcomes in aged mice. J. Gerontol. A Biol. Sci. Med. Sci. **64**:940–948.
18. **Lee SJ.** 2004. Regulation of muscle mass by myostatin. Annu. Rev. Cell Dev. Biol. **20**:61–86.
19. **Lee SJ, McPherron AC.** 2001. Regulation of myostatin activity and muscle growth. Proc. Natl. Acad. Sci. U. S. A. **98**:9306–9311.
20. **Lee SJ, et al.** 2005. Regulation of muscle growth by multiple ligands signaling through activin type II receptors. Proc. Natl. Acad. Sci. U. S. A. **102**:18117–18122.
21. **Lustig Y, et al.** 2011. Separation of the gluconeogenic and mitochondrial functions of PGC-1{alpha} through S6 kinase. Genes Dev. **25**:1232–1244.
22. **McPherron AC.** 2010. Metabolic functions of myostatin and GDF11. Immunol. Endocr. Metab. Agents Med. Chem. **10**:217–231.
23. **McPherron AC, Lee SJ.** 2002. Suppression of body fat accumulation in myostatin-deficient mice. J. Clin. Invest. **109**:595–601.
24. **Mukherjee A, et al.** 2007. FSTL3 deletion reveals roles for TGF-beta family ligands in glucose and fat homeostasis in adults. Proc. Natl. Acad. Sci. U. S. A. **104**:1348–1353.
25. **Nedergaard J, Bengtsson T, Cannon B.** 2007. Unexpected evidence for active brown adipose tissue in adult humans. Am. J. Physiol. Endocrinol. Metab. **293**:E444–E452.
26. **Nedergaard J, Cannon B.** 2010. The changed metabolic world with human brown adipose tissue: therapeutic visions. Cell Metab. **11**:268–272.
27. **Newton MA, Quintana FA, Denboon JA, Sengupta S, Ahlquist P.** 2007. Random-set methods identify distinct aspects of the enrichment signal in gene-set analysis. Ann. Appl. Stat. **1**:85–106.
28. **Ordway GA, Garry DJ.** 2004. Myoglobin: an essential hemoprotein in striated muscle. J. Exp. Biol. **207**:3441–3446.
29. **Puigserver P, et al.** 1998. A cold-inducible coactivator of nuclear receptors linked to adaptive thermogenesis. Cell **92**:829–839.
30. **Rebbapragada A, Benchabane H, Wrana JL, Celeste AJ, Attisano L.** 2003. Myostatin signals through a transforming growth factor beta-like signaling pathway to block adipogenesis. Mol. Cell. Biol. **23**:7230–7242.
31. **Schulz TJ, Tseng YH.** 2009. Emerging role of bone morphogenetic proteins in adipogenesis and energy metabolism. Cytokine Growth Factor Rev. **20**:523–531.
32. **Seale P, et al.** 2008. PRDM16 controls a brown fat/skeletal muscle switch. Nature **454**:961–967.
33. **Seale P, et al.** 2007. Transcriptional control of brown fat determination by PRDM16. Cell Metab. **6**:38–54.
34. **Subramanian A, et al.** 2005. Gene set enrichment analysis: a knowledge-based approach for interpreting genome-wide expression profiles. Proc. Natl. Acad. Sci. U. S. A. **102**:15545–15550.
35. **Tan CK, et al.** 2011. Smad3 deficiency in mice protects against insulin resistance and obesity induced by a high-fat diet. Diabetes **60**:464–476.
36. **Timmons JA, et al.** 2007. Myogenic gene expression signature establishes that brown and white adipocytes originate from distinct cell lineages. Proc. Natl. Acad. Sci. U. S. A. **104**:4401–4406.
37. **Trendelenburg AU, et al.** 2009. Myostatin reduces Akt/TORC1/p70S6K signaling, inhibiting myoblast differentiation and myotube size. Am. J. Physiol. Cell Physiol. **296**:C1258–C1270.
38. **Tseng YH, et al.** 2008. New role of bone morphogenetic protein 7 in brown adipogenesis and energy expenditure. Nature **454**:1000–1004.
39. **Uldry M, et al.** 2006. Complementary action of the PGC-1 coactivators in mitochondrial biogenesis and brown fat differentiation. Cell Metab. **3**:333–341.
40. **van Marken Lichtenbelt WD, et al.** 2009. Cold-activated brown adipose tissue in healthy men. N. Engl. J. Med. **360**:1500–1508.
41. **Vernochet C, McDonald ME, Farmer SR.** 2010. Brown adipose tissue: a promising target to combat obesity. Drug News Perspect. **23**:409–417.
42. **Virtanen KA, et al.** 2009. Functional brown adipose tissue in healthy adults. N. Engl. J. Med. **360**:1518–1525.
43. **Waters DL, Baumgartner RN.** 2011. Sarcopenia and obesity. Clin. Geriatr. Med. **27**:401–421.
44. **Whittemore LA, et al.** 2003. Inhibition of myostatin in adult mice increases skeletal muscle mass and strength. Biochem. Biophys. Res. Commun. **300**:965–971.
45. **Yadav H, et al.** 2011. Protection from obesity and diabetes by blockade of TGF-beta/Smad3 signaling. Cell Metab. **14**:67–79.
46. **Zamani N, Brown CW.** 2011. Emerging roles for the transforming growth factor-{beta} superfamily in regulating adiposity and energy expenditure. Endocr. Rev. **32**:387–403.
47. **Zamboni M, Mazzali G, Fantin F, Rossi A, Di Francesco V.** 2008. Sarcopenic obesity: a new category of obesity in the elderly. Nutr. Metab. Cardiovasc. Dis. **18**:388–395.
48. **Zhang C, et al.** 2011. Myostatin-deficient mice exhibit reduced insulin resistance through activating the AMP-activated protein kinase signalling pathway. Diabetologia **54**:1491–1501.